Dalton Transactions

PAPER

View Article Online
View Journal | View Issue

Cite this: *Dalton Trans.*, 2015, **44**, 4498

Pressure-induced oversaturation and phase transition in zeolitic imidazolate frameworks with remarkable mechanical stability†

Pu Zhao,[a] Thomas D. Bennett,[b] Nicola P. M. Casati,[c] Giulio I. Lampronti,[a] Stephen A. Moggach[d] and Simon A. T. Redfern*[a]

Received 2nd September 2014,
Accepted 23rd January 2015

DOI: 10.1039/c4dt02680b

www.rsc.org/dalton

Zeolitic imidazolate frameworks (ZIFs) 7 and 9 are excellent candidates for CO_2 adsorption and storage. Here, high-pressure X-ray diffraction is used to further understand their potential in realistic industrial applications. ZIF-7 and ZIF-9 are shown be able to withstand high hydrostatic pressures whilst retaining their porosity and structural integrity through a new ferroelastic phase transition. This stability is attributed to the presence of sterically large organic ligands. Results confirm the notable influence of guest occupancy on the response of ZIFs to pressure; oversaturation of ZIFs with solvent molecules greatly decreases their compressibility and increases their resistance to amorphisation. By comparing the behaviours of both ZIFs under high pressure, it is demonstrated that their mechanical stability is not affected by metal substitution. The evacuated ZIF-7 phase, ZIF-7-II, is shown to be able to recover to the ZIF-7 structure with excellent resistance to pressure. Examining the pressure-related structural behaviours of ZIF-7 and ZIF-9, we have assessed the great industrial potential of ZIFs.

Introduction

Atmospheric CO_2 is the primary anthropogenic greenhouse gas and much recent attention has focused on engineering solutions for its capture and storage. In fuel-burning exhaust streams, gaseous CO_2 is often sequestered by alkaline solutions or solids. Such processes, however, typically require high temperature and/or pressure and are characterised by high energy consumption. Microporous solid hosts have recently been proposed as lower-energy alternatives for CO_2 capture. Of these, zeolitic imidazolate frameworks (ZIFs) are outstanding candidates due to their excellent CO_2 adsorption capacity and selectivity.

ZIF-7 ($Zn(PhIm)_2$, PhIm: benzimidazolate, $C_7H_5N_2^-$) and its cobalt-substituted equivalent ZIF-9, attract considerable interest. They adopt the sodalite (SOD) structural topology and have trigonal symmetry $R\bar{3}$ (a = 22.989(3) Å, c = 15.763(3) Å, V = 7214(2) Å^3) (Fig. 1).[1] ZIF-7 undergoes a reversible displacive phase transition induced by pore-occupation by guest molecules such as CO_2, which accounts for the "gate-opening" behaviour seen in its CO_2 adsorption process.[2,3] The low-symmetry distorted phase ZIF-7-II, produced upon evacuating ZIF-7, has triclinic symmetry $P\bar{1}$ (a = 23.948(6) Å, b = 21.354(6) Å, c = 16.349(4) Å, α = 90.28(2)°, β = 93.28(2)°, γ = 108.41(1)°, V = 7917(3) Å^3). Previously, we studied CO_2 adsorption geometry in ZIF-7.[4] We noticed that at relatively high loading pressure, CO_2 adsorption is prohibited because squeezed pores in the host material were no longer able to uptake any more CO_2 molecule; CO_2 adsorption in ZIF-7 is dependent on a balance between the internal pressure of the guest molecules and the

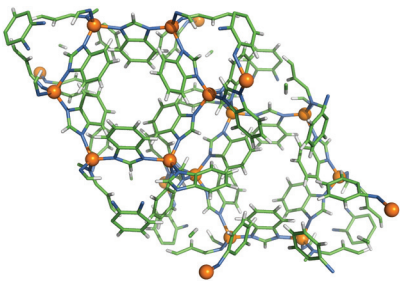

Fig. 1 The unit cell of ZIF-7 and ZIF-9. Zn/Co: orange, C: green, N: blue, H: silver.

[a]*Department of Earth Sciences, University of Cambridge. Downing Street, Cambridge, CB2 3EQ, UK. E-mail: satr@cam.ac.uk*
[b]*Department of Materials Science and Metallurgy, University of Cambridge, 27 Charles Babbage Road, Cambridge, CB3 0FS, UK*
[c]*Paul Scherrer Institut, 5232 Villigen PSI, Switzerland*
[d]*School of Chemistry, University of Edinburgh, West Mains Road, Edinburgh, EH9 3JJ, UK*

†Electronic supplementary information (ESI) available: Sample synthesis and characterisation, analysis details, structure solution and refinement methods, crystallographic data. CCDC 1036075–1036079. For ESI and crystallographic data in CIF or other electronic format see DOI: 10.1039/c4dt02680b

external gas pressure imposed. Here we further investigate the influence of external confining pressure on the properties of ZIF-7 and ZIF-9, and compare the relative influence of external pressure and internal pressure given by guest molecules on their structural response. Such pressures correspond to those expected during industrial gas adsorption and separation processes (*e.g.* pre/post-combustion CO_2 capture: 5–15 MPa),[5,6] as well as in, for example, high-pressure liquid chromatography (14–140 MPa).[7] A wide pressure range (up to 5.65 GPa) was studied to allow us to thoroughly examine the pressure-dependent behaviours of ZIF-7 and ZIF-9.

Despite their industrial potential and extensive research on the family, there are only a handful of high-pressure structural studies of ZIFs, employing either single-crystal or powder X-ray diffraction. Spencer *et al.* first examined dense $Zn(Im)_2$ (or ZIF-zni,[8] Im: imidazolate, $C_3H_3N_2^-$).[9] They obtained a bulk modulus of 14 GPa and identified an irreversible phase transition driven by cooperative bond rearrangement (α-phase: $I4_1cd$ to β-phase: $I4_1$) in the pressure range 0.54–0.85 GPa. Later studies on microporous ZIF-8 ($Zn(mIm)_2$, mIm: 2-methylimidazolate, $C_4H_5N_2^-$, SOD topology) were conducted by Chapman *et al.*[10] and ourselves.[11] Pressurisation beyond 0.34 GPa in a non-penetrating pressure-transmitting fluid (PTF) fluorinert FC75 leads to irreversible amorphisation of ZIF-8 (commercially-available sample, presumably containing *N*,*N*′-dimethylformamide (DMF) solvent). Pressurisation induced by a penetrating PTF 4 : 1 (volume ratio) methanol and ethanol mixture (ME), however, gives rise to a reversible phase transition in methanol-containing sample at 1.47 GPa (ZIF-8: $I\bar{4}3m$ to ZIF-8-II: $I\bar{4}3m$), associated with a "gate-opening" phenomenon. A bulk modulus of 6.5 GPa was determined for commercially-available ZIF-8 sample. The pressure-related structural behaviour of ZIF-4 ($Zn(Im)_2$, cag topology), a framework of relatively low porosity, has also been studied.[12] In contrast to its irreversible transition to ZIF-zni upon heating,[13] ZIF-4 shows a phase transition (ZIF-4: *Pbca* to ZIF-4-I: $P2_1/c$) below 0.56 GPa when guest molecules (methanol) were present in its internal pores and pressurisation was induced by a penetrating PTF (ME). Both solvated and desolvated ZIF-4 show reversible amorphisation as a function of pressure. The bulk moduli of pore-occupied ZIF-4 and ZIF-4-I were estimated to be 7.7 and 16.5 GPa, respectively, significantly higher than that of the evacuated framework (2.6 GPa).

Previous studies of porous ZIF-4 and ZIF-8 demonstrate the crucial influence of guest molecules on ZIFs' mechanical properties. The fact that pore filling decreases compressibility and increases resistance to amorphisation has also been demonstrated in zeolites.[14,15] Both ZIF-4 and ZIF-8 frameworks are relatively simple in terms of ligand and crystal system (cubic and orthorhombic respectively) and have relatively small unit cells (V = 4300–4900 Å^3). Given suggestions that sterically large ligands confer stability to microporous structures,[16] the absence of any reports of the bulk moduli of open framework materials of this type is surprising. We address this deficit here by studying crystallographically and chemically more complex ZIF-7 and ZIF-9 to further explore the extreme conditions under which ZIFs retain their quintessential properties. This is also the first study of the influence of metal substitution on pressure-related behaviour of ZIFs.

Experimental

Synthesis

ZIF-7 and ZIF-9 were synthesised following previously reported methods.[1,2] The internal pores of the as-synthesised samples are initially occupied with DMF solvent molecules; though these can be exchanged with another small-molecule organic solvent or removed by heating which introduces the phase transition from ZIF-7 to ZIF-7-II.[2]

High-pressure X-ray powder diffraction. HP-XRPD experiments were conducted at beamline X04SA of Swiss Light Source.[17] They were used to study the structural responses of ZIF-7 samples containing DMF (experiments A and B), ME (experiment C) and evacuated (ZIF-7-II, experiment D) with both small-molecule PTFs (DMF in experiment A; ME in experiment C) and large-molecule PTF (1 : 1 (volume ratio) fluorinert FC770 and FC75 mixture (FC) in experiments B and D).

Data collection was performed using a 1D MYTHEN II microstrip detector.[18] The working photon wavelength was calibrated using a silicon standard (NIST 640C) (λ = 0.70850 Å). Pressures were applied to the sample using a gas-membrane Boehler-type diamond anvil cell (DAC, 500 μm diamond culets). The sample pressure was measured using the equation of state (EoS) of quartz which was loaded in the DAC as the internal standard.[19] The pressure step size was 0.01 GPa in the range of 0 to 1 GPa; for high pressures above 1 GPa, it varied from 0.1 to 1 GPa. After each experiment, pressure was released from the DAC gradually. Diffraction data were recorded while pressure decreased and at ambient pressure. The raw data were processed and merged using in-house software. Pawley fitting was used to extract the unit cell parameters of ZIF-7 as a function of pressure, with the programme TOPAS-Academic 4.1.[20,21]

High-pressure single-crystal X-ray diffraction. Single-crystal XRD data of a DMF-containing ZIF-9 sample were collected on a Bruker APEX II diffractometer with graphite-monochromated Mo Kα radiation (λ = 0.71073 Å) at 0.91, 1.78, 2.74, 3.54, 4.14, 4.67 and 5.27 GPa in a small-molecule PTF (ME, experiment E). Pressures were applied using a modified Merrill-Bassett DAC (600 μm diamond culets) and a tungsten gasket.[22] The sample and a chip of ruby (as a pressure calibrant) were loaded into the DAC with ME. The ruby fluorescence method was utilised to measure the pressure.[23] Data were collected in ω-scans in twelve settings of 2θ and ϕ with a frame and step size of 40 s and 0.3° respectively. Data were integrated by the programme SAINT.[24] Absorption corrections for the DAC and sample were carried out with the programmes SHADE[25] and SADABS[26] respectively. Structural refinement was carried out against $|F|^2$ using the programme CRYSTALS.[27] The solvent content was calculated using the SQUEEZE algorithm within PLATON.[28]

Results and discussion

Experiment A: ZIF-7 (DMF) in DMF

Pressures between 0 and 1.01 GPa were applied to an as-synthesised ZIF-7 sample using DMF as a PTF. DMF has similar molecular weight, density, kinematic viscosity and vapour pressure to commonly-used alkane-based PTFs whose hydrostatic pressure limits exceed 6 GPa;[29] it is therefore anticipated that all modest pressures in Experiment A are hydrostatic.[30] Several diffraction peaks split upon increasing pressure, indicating that a symmetry reduction in ZIF-7 had taken place (Fig. 2). To investigate the effect of this symmetry reduction on the primary guest-hosting internal pore,[2,4] diffraction patterns were fitted using a primitive triclinic unit cell based on the ZIF-7 rhombohedral unit cell ($a = b = c = 14.247$ Å, $\alpha = \beta = \gamma = 107.23°$).

At the lowest pressures (0.02–0.05 GPa), the unit cell volume increases continuously with pressure (Fig. 3). This is related to the incorporation of DMF molecules migrating from the PTF into the framework as pressure rises. A similar oversaturation phenomenon under pressure has been observed previously in ZIF-8[11] and is known in zeolites.[31] For pressures above 0.05 GPa the volume-pressure relation was fitted with a second-order Birch-Murnaghan EoS (Fig. 4 in the (ESI†)),[9,31,32] giving a bulk modulus (K_{0A}) of 23.3(5) GPa at ambient temperature. The highest bulk modulus previously reported for ZIF-related materials is 16.6 GPa for $LiB(Im)_4$, a dense analogue of ZIF-zni, though there was no solvent present.[33] Pore penetration by PTF gives ZIF-7 the lowest compressibility found in ZIF materials yet. It should be noted that aluminosilicate zeolites typically show K_0 in the range 14–70 GPa;[9,16,31] the bulk mechanical properties of ZIFs appear to be approaching the regime of their inorganic analogues. This highlights the mechanical stability of ZIFs and underlines their huge potential in industrial application.

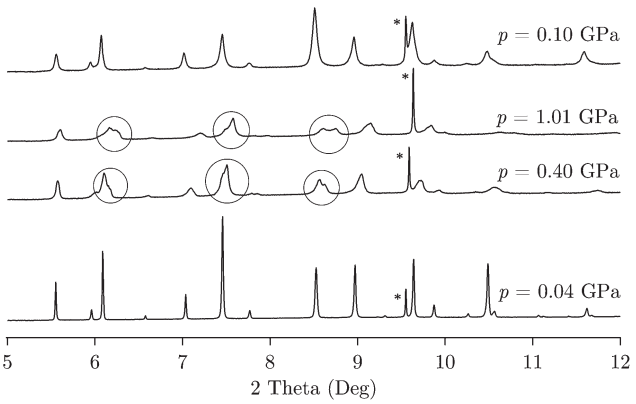

Fig. 2 X-ray diffraction peak splitting upon increasing pressure and recovery at low pressure in Experiment A. The diffraction peak from quartz standard is indicated by *.

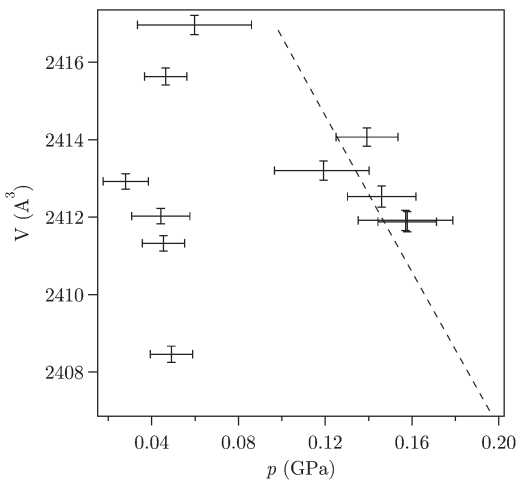

Fig. 3 Pressure-induced oversaturation reflected by an increase in volume upon pressurisation at low pressure. Dashed line is the EoS fit at higher pressure.

In order to understand the pressure-induced symmetry-breaking phase transition seen in Fig. 2, the ferroelastic spontaneous strains (S) were calculated at each pressure and their pressure evolution was characterised by fitting an effective order parameter S with critical exponent n:

$$S = A(p - p_c)^n \quad (1)$$

where p is the pressure of measurement and p_c is the phase transition critical pressure; A is a material constant and n is the critical exponent for the phase transition. Spontaneous strains were defined as:

$$S_0 = 3(a - c)/(a + b + c) \quad (2)$$

$$S_1 = (\alpha - \gamma) \quad (3)$$

Fits give a critical pressure, p_c = 0.02–0.05 GPa, at which point ZIF-7 transforms to a previously unknown high-pressure *para*-elastic phase with triclinic symmetry (denoted ZIF-7-IV). Rietveld refinement,[34] using the ZIF-7 rhombohedral structure as a starting model, of data collected at p = 0.40 GPa was carried out to obtain the low-symmetry ZIF-7-IV structure. The metal tetrahedral topology, structural connectivity and porosity in ZIF-7 are retained in the new phase. Moderate structural distortion in the primary guest-hosting internal pore leads to the symmetry loss seen in ZIF-7-IV ($P\bar{1}$). Calculations using the programme Mercury[35] show a slight increase in the percentage of the void in the unit cell on increasing pressure through this phase transition, from 23.2% in ZIF-7 to 25.5% in ZIF-7-IV. The phase transition pressure is intriguingly low compared to that of methanol-containing ZIF-4 (0.56 GPa)[12] and ZIF-8 (1.47 GPa)[11] in a ME PTF. We attribute this to the sterical effect of the benzimidazolate ligands. ZIF-7-IV is stable up to 1.01 GPa. The ZIF-7 to ZIF-7-IV transition is displacive and reversible, with the ZIF-7 trigonal aristotype structure fully recovered by the same ferroleastic transition on depressurisation (Fig. 2).

Experiment B: ZIF-7 (DMF) in FC

FC was used as a non-penetrating external pressure-transmitting medium to exert pressures between 0 and 3.44 GPa on the

Table 1 Summary of the pressure-dependent behaviour of ZIF-7 in Experiment A–C

Sample		PTF	p_c [a] (GPa)	Amorphisation pressure (GPa)	K_0 [b] (GPa)
ZIF-7(DMF)	A	DMF	0.02–0.05		23.3(5)
	B	FC	-2.4×10^{-9}	3.45	13(1)
ZIF-7(ME)	C	ME		5.65	21.1(7)

[a] p_c: the critical pressure of the phase transition from ZIF-7 to ZIF-7-IV. [b] K_0: the bulk modulus of ZIF-7/ZIF-7-IV.

as-synthesised ZIF-7. The hydrostatic pressure limit of this fluorinert mixture is reported as 1.2–1.5 GPa.[30,36] Data collected beyond this limit were not fitted and non-hydrostaticity was confirmed by the divergence of Pawley fits. In contrast to Experiment A, no initial cell expansion was seen at the onset of pressurisation. This supports the conclusion that the initial increase in volume seen in Experiment A is due to the incorporation of DMF into the framework. There is a turning point around p = 0.5–0.6 GPa in the volume-pressure data (Fig. 6, ESI†), which may indicate another phase transition, though a full structural refinement was not possible from the powder data at this pressure. Two separate second-order Birch-Murnaghan EoSs were used to fit data in the pressure ranges 0–0.5 and 0.5–1.5 GPa, giving two bulk moduli K_{0B} = 13(1) GPa (ZIF-7-IV) and K'_{0B} = 22(2) GPa. Both values are significantly larger than those of the bulk moduli of as-synthesised and high-pressure phases of ZIF-4 (methanol-containing) in a penetrating PTF (ME) (7.7 and 15 GPa respectively).[12] The difference in moduli between Experiment A (K_{0A}) and B (K_{0B}) is attributed to the oversaturation of ZIF-7 with DMF in the former, which decreases its compressibility.[37,38] When the critical pressures of the ZIF-7 to ZIF-7-IV phase transition are compared (Table 1), one notices that ZIF-7-IV appears as soon as pressure is applied in Experiment B. This is because the non-penetrating PTF exerts a much stronger external pressure on ZIF-7. *In situ* reversible amorphisation of ZIF-7 was observed in Experiment B at a (comparatively) high pressure of 3.45 GPa. Given the reversible nature of the transition and by analogy with unsubstituted ZIF-4, we anticipate that short-range ordering and associated structural connectivity of ZIF-7 are unaffected by pressure.[12]

Experiment C and D: ZIF-7-II in ME and FC

To further investigate the effect of guest occupancy upon pressure-related behaviour, we repeated Experiment A and B with evacuated samples of ZIF-7, "ZIF-7-II", in Experiment C and D. Small-molecule PTF ME and large-molecule PTF FC were used respectively. ZIF-7-II was prepared by heating ZIF-7 at 400 K in air for 24 h. In Experiment C, ZIF-7-II transformed back to ZIF-7 as soon as ME was loaded at ambient pressure, suggesting that primary guest-hosting pores were filled by methanol and/or ethanol molecules, as previously reported.[2] Pressures between 0 and 5.65 GPa were then applied to this methanol/ethanol-bearing ZIF-7. The phase transition from ZIF-7 to ZIF-7-IV was observed, however, a meaningful estimate of the critical pressure could not be obtained due to poor data coverage between 0.2 and 0.9 GPa. Using a second-order Birch-Murnagan EoS we obtain a bulk modulus K_{0C} = 21.1(7) GPa, consistent with K_{0A}. Although the Bragg peaks at 5.65 GPa were too broad to yield precise cell parameters, it is clear that ZIF-7-IV remains stable to this pressure. This is exceptionally interesting in view of the CO_2 adsorption ability of ZIF-7; its competency to retain high porosity at relatively high-pressure gives possibilities for carbon capture applications at such conditions. In Experiment D, ZIF-7-II retained its structure since FC is not able to penetrate. ZIF-7-II has poor crystallinity characterised by broad Bragg peaks. It appeared to show structural collapse at a very early stage on pressurisation and was damaged at 4.54 GPa.

The higher amorphisation pressure of ZIF-7-IV in Experiment C (compared with that in Experiment B) also indicates that the penetration of PTF molecules plays an important role in the high-pressure stability of ZIF structures. The recovered ZIF-7 or ZIF-7-IV cell was measured on pressure release back to ambient. The reversal of the ZIF-7 to ZIF-7-IV phase transition was difficult to identify due to the very low pressure of the transition, pressure hysteresis in the DAC and excessive peak broadening after amorphisation. Our observations demonstrate the excellent recovery from ZIF-7-II to ZIF-7 and the exceptional resilience to pressure of the recovered structure. Bearing this in mind, realistic gas sequestration applications of ZIF-7 could exploit pore activation, performed by mild heating, without concerns about degradation of the recovered structure.

Experiment E: ZIF-9 (DMF) in ME

ZIF-9 ($Co(PhIm)_2$) is isostructural with ZIF-7 and allows us to explore the role of metal substitution (Co for Zn). The study is the first high-pressure experiment performed on a Co-based ZIF. Previously, metal substitution in dense ZIF-zni (Zn^{2+} compared with alternating Li^+ and B^{3+} cations) revealed small changes in bulk modulus: 14 and 16.6 GPa for ZIF-zni and BIF-1-Li respectively.[33] The lower compressibility of the latter is consistent with its smaller porosity. ZIF-9 is only slightly denser than ZIF-7 and the difference in porosity between the two structures is very small.[39] Density and porosity differences should not have a great effect on our conclusions regarding metal substitution. Whilst phase-pure powders of ZIF-9 could not be prepared, single crystal samples were available and a single-crystal high-pressure diffraction study was performed on a DMF-containing ZIF-9. Data were collected at 0.91, 1.78, 2.74 and 3.54 GPa using ME as a PTF. After attaining a structural refinement at 3.54 GPa, the decrease in data quality rendered further refinements impossible, though lattice parameters were recorded at 4.14, 4.67 and 5.27 GPa (Table 1, ESI†). The lack of low-pressure data prohibits commentary on any pressure-induced phase transition equivalent to that of ZIF-7 to ZIF-7-IV. A second order Birch-Murnaghan EoS was fitted, yielding a bulk modulus (K_{0E}) of 13.4(5) GPa (Fig. 4). This is similar in magnitude as that of ZIF-zni and of ZIF-7 in Experiment B. Above 5.27 GPa, the gasket containing the crystal

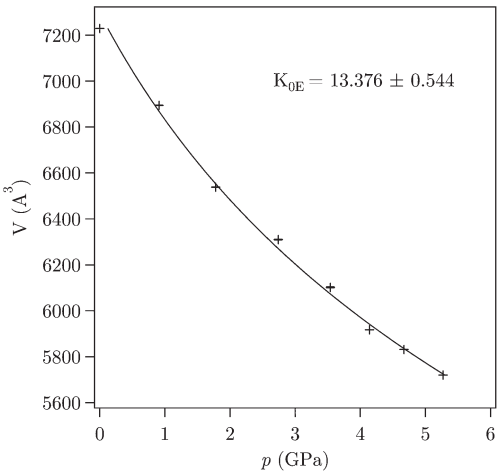

Fig. 4 The evolution of the unit cell volume of ZIF-9 as a function of hydrostatic pressure, completed with EoS fit.

failed, although the crystal itself remained intact. The survival of the single crystal to such high pressures is comparable to the case of ZIF-7, and suggests the general retention of stability to pressure upon metal center replacement.

Attempted evacuation of the singe crystal of ZIF-9 led to significant cracking, and this, combined with the absence of a phase pure powder sample, meant that the presence/absence of a structural transition upon evacuation, analogous to that of ZIF-7 to ZIF-7-II,[2] remains to be investigated. Structural refinements did not give any indication that a structural transition had taken place. The absence of low pressure data is indicative of the inherent difficulties of controlling the application of pressure in single-crystal experiments. The entrance of methanol molecules into the framework was observed between 0 and 1.78 GPa (Table 1, ESI†), which may indicate oversaturation of the framework, though more pressure points would be needed to confirm the effect.

Conclusions

In summary, we have shown that ZIF-7 and ZIF-9 can withstand high hydrostatic pressures, whilst retaining their porosity and structural integrity. Structural response to pressure includes a ferroelastic phase transition to a distorted but stable and topologically invariant high-pressure phase. This stability is attributed to the presence of sterically large organic ligands which confer mechanical stability to the framework. Our results confirm the influence of guest occupancy on the response of ZIFs to pressure. Notably, the oversaturation of ZIFs with solvent molecules greatly decreases their compressibility and increases their resistance to amorphisation. The oversaturation and phase transition pressures we observed in Experiment A are consistent with those in industrial carbon capture processes, it would be of interest to investigate the structural response of ZIFs under supercritical fluid of CO_2 (*e.g.* 10 MPa, 323 K) in future studies.

A comparison of the behaviours of ZIF-7 and ZIF-9 under high pressure demonstrates that their mechanical stability is unaffected by metal substitution. The evacuated ZIF-7 phase, ZIF-7-II, can easily recover to ZIF-7 structure by guest reoccupation. The recovered structure shows excellent pressure resilience. The pressure-dependent structural behaviours of ZIF-7 and ZIF-9 indicate the encouraging potential of ZIFs in realistic industrial applications.

Acknowledgements

This work was supported by the Cambridge Commonwealth, European and International Trust; China Scholarship Council; Trinity Hall, University of Cambridge; UK Science & Technology Facilities Council. We thank anonymous reviewers for their valuable suggestions on the improvement of this manuscript.

Notes and references

1 K. S. Park, Z. Ni, A. P. Côté, J. Y. Choi, R. Huang, F. J. Uribe-Romo, H. K. Chae, M. O'Keeffe and O. M. Yaghi, *Proc. Natl. Acad. Sci. U. S. A*, 2006, **103**, 10186–10191.
2 P. Zhao, G. I. Lampronti, G. O. Lloyd, M. T. Wharmby, S. Facq, A. K. Cheetham and S. A. T. Redfern, *Chem. Mater.*, 2014, **26**, 1767–1769.
3 S. Aguado, G. Bergeret, M. P. Titus, V. Moizan, C. Nieto-Draghi, N. Bats and D. Farrusseng, *New J. Chem.*, 2011, **35**, 546–550.
4 P. Zhao, G. I. Lampronti, G. O. Lloyd, E. Suard and S. A. T. Redfern, *J. Mater. Chem. A*, 2014, **2**, 620–623.
5 J. Y. Jung, F. Karadas, S. Zulfiqar, E. Deniz, S. Aparicio, M. Atilhan, C. T. Yavuz and S. M. Han, *Phys. Chem. Chem. Phys.*, 2013, **15**, 14319–14327.
6 The National Energy Technology Laboratory (NETL), http://www.netl.doe.gov/research/coal/carbon-capture, accessed January 2015.
7 *Syringe Pump Application Note AN6 High Pressure Liquid Chromatography*, Teledyne Isco Inc., 2012, http://www.isco.com/WebProductFiles/Applications/105/Application_Notes/HPLC_System_Configuration.pdf, accessed January 2015.
8 R. Lehnert and F. Seel, *Z. Anorg. Allg. Chem.*, 1980, **464**, 187–194.
9 E. C. Spencer, R. J. Angel, N. L. Ross, B. E. Hanson and J. A. K. Howard, *J. Am. Chem. Soc.*, 2009, **131**, 4022–4026.
10 K. W. Chapman, G. J. Halder and P. J. Chupas, *J. Am. Chem. Soc.*, 2009, **131**, 17546–17547.
11 S. A. Moggach, T. D. Bennett and A. K. Cheetham, *Angew. Chem., Int. Ed.*, 2009, **48**, 7087–7089.
12 T. D. Bennett, P. Simoncic, S. A. Moggach, F. Gozzo, P. Macchi, D. A. Keen, J. C. Tan and A. K. Cheetham, *Chem. Commun.*, 2011, **47**, 7983–7985.

13 T. D. Bennett, D. A. Keen, J. C. Tan, E. R. Barney, A. L. Goodwin and A. K. Cheetham, *Angew. Chem., Int. Ed.*, 2011, **123**, 3123–3127.
14 B. Coasne, J. Haines, C. Levelut, O. Cambon, M. Santoro, F. Gorelli and G. Garbarino, *Phys. Chem. Chem. Phys.*, 2011, **13**, 20096–20099.
15 J. Haines, O. Cambon, C. Levelut, M. Santoro, F. Gorelli and G. Garbarino, *J. Am. Chem. Soc.*, 2010, **132**, 8860–8886.
16 J. C. Tan and A. K. Cheetham, *Chem. Soc. Rev.*, 2011, **40**, 1059–1080.
17 P. R. Willmott, D. Meister, S. J. Leake, M. Lange, A. Bergamaschi, M. Böge, M. Calvi, C. Cancellieri, N. Casati, A. Cervellino, *et al.*, *J. Synchrotron Radiat.*, 2013, **20**, 667–682.
18 A. Bergamaschi, A. Cervellino, R. Dinapoli, F. Gozzo, B. Henrich, I. Johnson, P. Kraft, A. Mozzanica, B. Schmitt and X. Shi, *J. Synchrotron Radiat.*, 2010, **17**, 653–668.
19 R. J. Angel, D. R. Allan, R. Miletich and L. W. Finger, *J. Appl. Crystallogr.*, 1997, **30**, 461–466.
20 A. A. Coelho, *Coelho Software, 4.1 ed*, Brisbane, 2007.
21 G. Pawley, *J. Appl. Crystallogr.*, 1981, **14**, 357–361.
22 S. A. Moggach, D. R. Allan, S. Parsons and J. E. Warren, *J. Appl. Crystallogr.*, 2008, **41**, 249–251.
23 G. J. Piermarini, S. Block, J. D. Barnett and R. A. Forman, *J. Appl. Phys.*, 1975, **46**, 2774–2780.
24 A. Dawson, D. R. Allan, S. Parsons and M. Ruf, *J. Appl. Crystallogr.*, 2004, **37**, 410–416.
25 S. Parsons, *SHADE*, the University of Edinburgh, Edinburgh, UK, 2004.
26 G. M. Sheldrick, *SADABS*, 2004.
27 P. W. Betteridge, J. R. Carruthers, R. I. Cooper, K. Prout and D. J. Watkin, *J. Appl. Crystallogr.*, 2003, **36**, 1487.
28 A. L. Spek, *PLATON*, Utrecht University, Utrecht, the Netherlands, 2004.
29 S. Klotz, J. C. Chervin, P. Munsch and G. L. Marchand, *J. Phys. D: Appl. Phys.*, 2009, **42**, 075413.
30 V. A. Sidorov and R. A. Sadykov, *J. Phys.: Condens. Matter*, 2005, **17**, S3005–S3008.
31 G. D. Gatta and Y. Lee, *Mineral. Mag.*, 2014, **78**, 267–291.
32 R. J. Angel, in *Transformation process in minerals*, ed. S. A. T. Redfern and M. A. Carpenter, Mineralogical Society of America and Geochemical Society, Washington, DC, USA, 2000, vol. 39, pp. 85–104.
33 T. D. Bennett, J. C. Tan, S. A. Moggach, R. Galvelis, C. Mellot-Draznieks, B. A. Reisner, A. Thirumurugan, D. R. Allan and A. K. Cheetham, *Chem. – Eur. J*, 2010, **16**, 10684–10690.
34 R. A. Young, *The Rietveld Method*, Oxford University Press, 1995.
35 C. F. Macrae, I. J. Bruno, J. A. Chisholm, P. R. Edgington, P. McCabe, E. Pidcock, L. Rodriguez-Monge, R. Taylor, J. van de Streek and P. A. Wood, *J. Appl. Crystallogr.*, 2008, **41**, 466–470.
36 T. Varga, A. P. Wilkinson and R. J. Angel, *Rev. Sci. Instrum.*, 2003, **74**, 4564–4566.
37 A. U. Ortiz, A. Boutin, A. H. Fuchs and F. Coudert, *J. Phys. Chem. Lett.*, 2013, **4**, 1861–1865.
38 K. W. Chapman, G. J. Halder and P. J. Chupas, *J. Am. Chem. Soc.*, 2008, **130**, 10524–10526.
39 J. C. Tan, T. D. Bennett and A. K. Cheetham, *Proc. Natl. Acad. Sci. U.S.A.*, 2010, **107**, 9938–9943.